Residual Stress Analysis on High-Speed Face Milling of AA 7075-T6 Aluminium Alloy

[1]F.V. Díaz, [1]C.A. Mammana and [2]A.P.M. Guidobono
[1]Departamento de Ingeniería Electromecánica-Departamento de Ingeniería Industrial, Facultad Regional Rafaela, Universidad Tecnológica Nacional, Bvd Roca 989, 2300 Rafaela, Argentina
[2]División Metrología Dimensional, Centro Regional Rosario (INTI) Ocampo y Esmeralda, 2000 Rosario, Argentina

Abstract: The aim of this study is to investigate different states of residual stress generated by high-speed face milling in specimens of AA 7075-T6 aluminium alloy. The residual stresses are evaluated along the symmetry axes of the generated surfaces and also in the centroids corresponding to the conventional and climb cutting zones. An indentation method, based on the use of a universal measuring machine, is employed to determine the normal and shear components of residual stress. It is noteworthy that the use of this method makes possible to significantly reduce the absolute error of measurement. Different Mohr's circles are evaluated to compare the residual stress states introduced in the conventional and climb cutting zones. Finally, the results are analyzed in terms of mechanical and thermal effects generated in the primary cutting zone.

Keywords: Residual stresses, stress tensors, high-speed machining, face milling, aluminium alloy

INTRODUCTION

The growing interest in increasing productivity has driven the development of modern machining centers and new materials for tools, which in turn has made possible, in many metalmechanic industries, significant increases in the values of process parameters, transforming the conventional machining in High-Speed Machining (HSM) (Schulz, 1996). By using the latter, it is possible to reduce both the number of operations and time allocated to each of them. In addition, it is also possible to significantly improve the service of the cutting tools, which allows generating surfaces optimized in terms of geometry and roughness. However, it can occur that the distributions of residual stresses generated by this type of machining affect the service life of the machined components (Mantle and Aspinwall, 2001).

In this study, a recently developed method, based on the modification of the distance between two collinear indents (Wyatt and Berry, 2006), is used to determine different residual stress states, which were generated in specimens of AA 7075-T6 aluminium alloy milled at high speed. This method, which needs a Universal Measuring Machine (UMM), has the advantage of not requiring any specific equipment or highly skilled operators (Rendler and Vigness, 1966; Noyan and Cohen, 1987). Moreover, this method allows to measure residual displacements with an absolute error much smaller than those

corresponding to the traditional techniques (Diaz *et al.*, 2010; Diaz *et al.*, 2011).

The purpose of the present work is to investigate the residual stress states generated by HSM, with special attention to the role played by the thermal effects. High-speed tests consisted of face milling operations with central cutting. These operations were carried out in a numerically controlled vertical machining center. It is noteworthy that these operations with central cutting allow distinguishing in the generated surface, the conventional and climb cutting zones, which are adjacent. Low cutting speeds were also selected to evaluate the modification of residual stress tensors in those zones. To optimize the analysis, different Mohr's circles (Gere, 2001) associated with those stress tensors were assessed. Finally, through the evaluation of thermal effects corresponding to the cutting mechanics, it was possible to identify the causes that generate the residual stress tensors introduced through different combinations of process parameters.

METHODOLOGY

Determination of residual stress components: As mentioned previously, the method used in this work is based on the change of distance between two collinear indents, which can be measured using a UMM. This change occurs when the surface residual stresses are

Corresponding Author: F.V. Diaz, Departamento de Ingenieria Electromecánica-Departamento de Ingeniería Industrial, Facultad Regional Rafaela, Universidad Tecnológica Nacional, Bvd Roca 989, 2300 Rafaela, Argentina Tel.: + 54 3492 432710; Fax: + 54 3492 422880
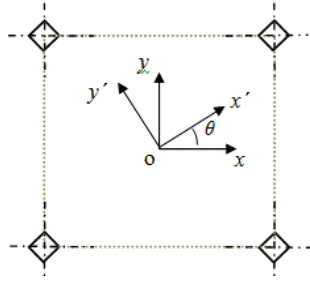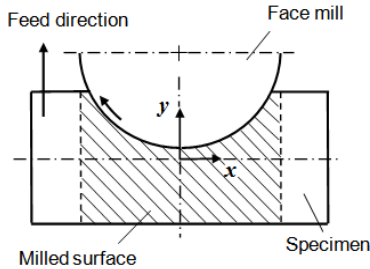
Fig. 1: Distribution of four indents

Fig. 2: Upper view of the specimen-tool system

released by a heat treatment (Wyatt and Berry, 2006). For example, through an indent distribution as shown in Fig. 1, it is possible to obtain the components of residual strain (Mammana *et al.*, 2010):

$$\varepsilon_x = \frac{l_x - l'_x}{l'_x}$$

$$\varepsilon_y = \frac{l_y - l'_y}{l'_y}$$

$$\varepsilon_d = \frac{l_d - l'_d}{l'_d}$$

$$\gamma_{xy} = 2 \cdot \varepsilon_d - \varepsilon_x - \varepsilon_y \qquad (1)$$

where l_x and l'_x are the mean values of the horizontal sides of the square and, l_y and l'_y are the mean values of the vertical sides, for both cases before and after the distension treatment, respectively. In turn, l_d and l'_d correspond to the positive slope diagonals of the square, also before and after the distension treatment, respectively. Then, assuming that the machined surface is under a plane stress state and also that the material is linearly elastic, homogeneous and isotropic, the residual stress components σ_x, σ_y and τ_{xy} can be obtained (Gere, 2001). Finally, the normal and shear components associated to an arbitrary direction θ (Fig. 1) can be evaluated through:

$$\sigma_{x'} = \frac{\sigma_x + \sigma_y}{2} + \frac{\sigma_x - \sigma_y}{2} \cdot \cos 2\theta + \tau_{xy} \cdot \sin 2\theta$$

$$\tau_{x'y'} = -\frac{\sigma_x - \sigma_y}{2} \cdot \sin 2\theta + \tau_{xy} \cdot \cos 2\theta \qquad (2)$$

It is important to note that the components of Eq. (2) can be represented by a graphical format known as Mohr's circle (Gere, 2001). This graphical representation is useful because it allows visualizing the relationships between normal and shear components corresponding to different orientations. Furthermore, this representation also allows viewing very clearly the variation ranges of those components.

Experimental procedure: This study was carried out by using a rolling product of AA 7075-T6 aluminium alloy. The optical microscopy revealed grains elongated in rolling direction (solid solution α, GS: 40 μm) with fine precipitated particles of $(Fe, Mn)Al_6$ and $CuMgAl_2$ aligned in this direction. The microhardness of this material is 186 HV0.5. Its chemical composition and mechanical characteristics are shown in Table 1. Regarding the maquinability, the rating of this alloy is B: curled or easily broken chips and good to excellent finish. It should be noted that A, B, C, D and E are relative ratings –for aluminium alloys– in increasing order of chip length and decreasing order of quality of finish (Chamberlain, 1979).

The dimensions of the tested specimens were 110 mm × 40 mm × 4 mm. Prior to the face milling tests, the specimens were heat treated to release the residual stresses generated by rolling. The temperature and time for the heat treatment were 573 K and 80 minutes respectively. For the milling tests, a self-balanced face mill of 63 mm in diameter was used, which incorporates five inserts (Palbit SEHT 1204 AFFN-AL SM10) of tungsten carbide. It is noteworthy that these inserts were designed especially for machining high strength aluminium alloys. In Table 2 both the geometry of the inserts and the process parameters selected for this study are detailed. Face milling tests were performed on a numerically controlled vertical machining center (Victor Vc-55). A superior view of the relative position of the tested specimen with respect to the cutting tool is shown in Fig. 2. Regarding the surface generated by milling, it is possible to distinguish the zones of conventional $(x > 0, y)$ and climb cutting $(x < 0, y)$.

The indentations were made using a Vickers micro hardness tester (Shimadzu HMV-2). The indent distribution introduced in the machined surface allowed assessing both the symmetry axes and the centroids of the

Table 1: Chemical composition and mechanical properties of the evaluated alloy

Chemical composition (wt %)								Mechanical properties		
Mg	Si	Mn	Fe	Cr	Zn	Cu	Al	σ_u (MPa)	$\sigma_{y0.2}$ (MPa)	A (%)
2.52	0.2	0.16	0.32	0.17	5.6	1.72	balance	564	506	11

Table 2: Tool geometry and process parameters

Rake angle	Clearance angle	Entrance angle	Cutting speed	Feed rate	Depth of cut
γ (°)	α (°)	χ (°)	V (m/min)	f (mm/rev)	d (mm)
45	7	45	100-1000	0.4-0.8	0.4

conventional and climb cutting zones. The distances between indents were obtained through measurements of the indent coordinates using a measuring machine GSIP MU-314. These measurements were carried out within a temperature range of 20 ± 0.2°C, with a variation rate less than 0.01°C/min. It is important to mention that if this rate is higher than the mentioned value, the measurement errors increase significantly. The distension treatment was carried out during 80 minutes at a temperature of 573 K. The error associated to the residual displacements was obtained through the absolute error corresponding to the distances between indents. First, the latter was evaluated taking into account the nominal and statistical measurement errors for a nominal distance of 28 mm (Diaz *et al.*, 2010; Diaz *et al.*, 2011). Then, by developing the probable absolute error equation (Taylor, 1997), the value corresponding to the error associated to such displacements was 1.5 µm.

RESULTS AND DISCUSSION

The normal components of the residual stress (σ_x, σ_y) were evaluated along the symmetry axes of the machined surface. Figure 3 shows the distributions obtained along the axis normal to the feed direction ($y = 0$). Although these components adopt very low values, the utilized technique allowed detecting the differences caused when the cutting speed or feed rate was modified. In all cases, the obtained values were compressive. The most striking feature of these distributions is that the change in cutting parameters did not alter the shape of them. It is important to note that the σ_y component shows a marked change of slope when the positive values of x are evaluated (conventional cutting zone).

To more clearly understand the different residual stress states introduced in the conventional and climb cutting zones, different Mohr's circles were analyzed. Figure 4 shows these circles, which correspond to the centroids of those zones. Note that the orthogonal coordinates of each point of each circle represent the values of residual stress components for an infinitesimal element whose axes are tilted at an angle θ with respect
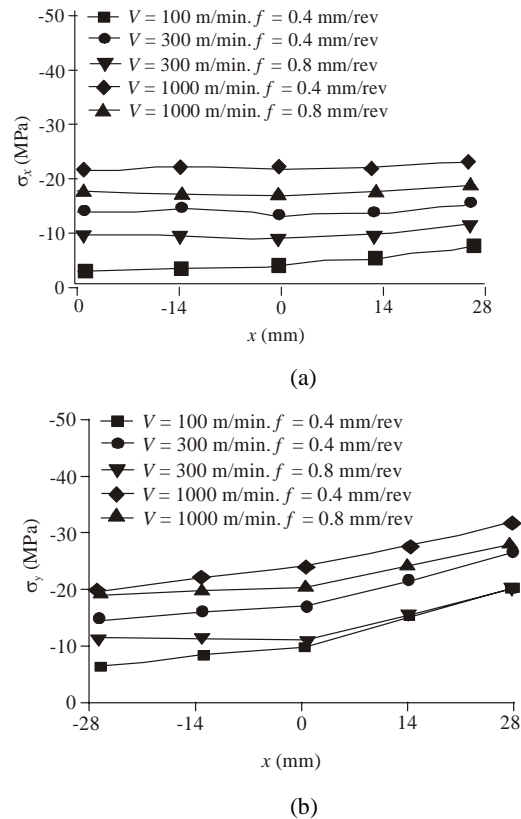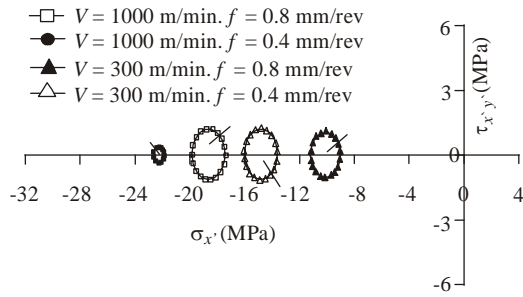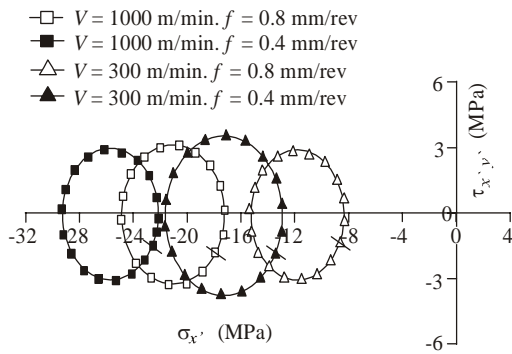

(a)

(b)

Fig. 3: Distributions of the components, (a) σ_x and, (b) σ_y of the residual stress along the axis $y = 0$

to the reference axes. Furthermore, the small segment of each circle defines the point corresponding to the reference direction ($\theta = 0$ in Fig. 1).

The circles shown in Fig. 4 a describe the stress states generated at the centroid of the climb cutting zone, where the component Vy of the cutting speed and feed rate f have the same direction. Both the arrangement and the diameters of the circles show that different combinations of process parameters generate homogeneous stress states where the normal component does not substantially change with the direction and, at the same time, the shear component shows very low values. In addition, the values of the normal component are more compressive when the cutting speed increases or feed rate decreases. On the other hand, Fig. 4 b shows the circles corresponding to the centroid of the conventional cutting zone, where the component Vy and feed rate f have opposite directions. Although the arrangement of these circles is similar to

(a)

(b)

Fig. 4: Mohr's circles corresponding to the barycentres of the (a) climb and (b) conventional cutting zones

the heat generation is doubled. Therefore, this time effect must be prevailing over the effect generated by the temperature in the primary cutting zone. However, this analysis should be extended to the fraction of heat transferred from the primary cutting zone to the workpiece, since the residual stresses depend on this incoming heat. This fraction of thermal energy can be expressed as (Özel and Zeren, 2004):

$$\beta = 0.5-0.35 \cdot \log (R_t \cdot \tan \phi) \text{ para } 0.04 \leq R_t \cdot \tan \phi \leq 10.0$$

$$\beta = 0.3-0.15 \cdot \log (R_t \cdot \tan \phi) \text{ para } R_t \cdot \tan \phi > 10.0 \quad (3)$$

where ϕ is the shear angle, $R_t = \rho \cdot S \cdot V \cdot d / K$, ρ is the density, S is the specific heat capacity and K is the thermal conductivity of the machined material. In terms of process parameters, R_t is only a function of the cutting speed and depth of cut. Therefore, the fraction of thermal energy β flowing to the work piece will be the same if the shear angle is similar for both feed rates. Considering that the variation of this angle with the feed rate is very small (Dhananchezian *et al.*, 2009), it is possible to conclude that the fraction of thermal energy β will be equivalent for both feed rates. Therefore, for the different combinations of process parameters selected in this study, the machining time effect will predominate in relation to the heat transfer to the work piece. Finally, in this heat transfer-and not in the cutting forces- it is possible to find the main cause of the different residual stress states generated in the evaluated material.

CONCLUSION

The indentation method used in this study proved to be very useful to determine with great precision residual stress components and tensors in surfaces generated by face milling. The analysis was carried out along the axes of symmetry of those surfaces and also in the centroids of the conventional and climb cutting zones. In all cases, the residual stresses caused by HSM were compressive and low. In addition, the distributions obtained did not change their shapes when the cutting speed or feed rate was modified. The residual stress tensors corresponding to the climb cutting zone were more homogeneous than those generated in the conventional cutting zone. Comparing both the distributions and tensors, the more compressive values were associated to the lower feed rate. This fact could be explained through the predominance-in terms of heat transferred to the workpiece– of the machining time effect over that corresponding to the temperature level in the primary cutting zone.

ACKNOWLEDGMENT

those shown in Fig. 4a, there are overlaps between them because the stress states generated are less homogeneous: the normal component shows greater variation with the direction changes and, at the same time, the shear component changes its value within a wider range.

An important aspect that emerges from both the stress distributions (Fig. 3) and Mohr's circles (Fig. 4) is the fact that the normal components are more compressive when the feed rate is lower for both cutting speeds. An analysis of this fact could help understand the causes generating the different residual stress states.

The cutting forces are higher when feed rate increases due to the augmentation of chip section (Yallese *et al.*, 2009). Therefore, the introduction of more compressive residual stresses when feed rate decreases may be a consequence of thermal effects. Regarding this item, it is well known that the cutting energy increases with the material removal rate (Hua *et al.*, 2005). Therefore, the temperature in the primary cutting zone (Trent, 1991) should augment if the feed rate increases. However, the heat transferred to the workpiece will also depend on the machining time. In our case, all specimens have the same dimensions. For this reason, the machining time will be different for each feed rate. When this rate is reduced by half (from 0.8 to 0.4 mm/rev), the time corresponding to

REFERENCES

Chamberlain, B., 1979. In: Metals Handbook-Properties and Selection: Nonferrous Alloys and Pure Metals. 9th Edn., ASME, 2: 187-190.

Dhananchezian, M., M. Pradeep Kumar and A. Rajadurai, 2009. Experimental investigation of cryogenic by liquid nitrogen in the orthogonal machining process. Int. J. Rec. Trends Eng., 1: 55-59.

Diaz, F.V., R. Bolmaro, A. Guidobono and E. Girini, 2010. Determination of residual stresses in high speed milled aluminium alloys using a method of indent pairs. Exp. Mech., 50: 205-215.

Diaz, F.V., C. Mammana, A. Guidobono and R. Bolmaro, 2011. Analysis of residual strain and stress distributions in high speed milled specimens using and indentation method. Int. J. Eng. Appl. Sci., 7: 40-46.

Gere, J.M., 2001. Mechanics of Materials. 5th Edn., Brooks/Cole, Pacific Grove, CA.

Hua, J., R. Shivpuri, X. Cheng, V. Bedekar, Y. Matsumoto, F. Hashimoto and T. Watkins, 2005. Effect of feed rate, work piece hardness and cutting edge on subsurface residual stress in the hard turning of bearing steel using chamfer+hone cutting edge geometry. Mater. Sci. Eng. A, 394: 238-248.

Mammana, C.A., F. Diaz, A. Guidobono and R. Bolmaro, 2010. Study of residual stress tensors in high-speed milled specimens of aluminium alloys using a method of indent pairs. Res. J. Appl. Sci. Eng. Technol., 2: 749-756.

Mantle, A.L. and D. Aspinwall, 2001. Surface integrity of a high speed milled gamma titanium aluminide. J. Mater. Proc. Tech., 118: 143-150.

Noyan, I.C. and J. Cohen, 1987. Residual stress measurement by diffraction and interpretation, Materials Research and Engineering. Springer Verlag, Berlin.

Özel, T. and E. Zeren, 2004. Determination of flow material stress and friction for FEA of machining using orthogonal cutting tests. J. Mater. Proc. Tech., 153: 1019-1025.

Rendler, N.J. and I. Vigness, 1966. Hole-drilling strain-gage method of measuring residual stresses. Exp. Mech., 6: 577-586.

Schulz, H., 1996. High Speed Machining. Carl Hanser, Munich.

Taylor, J.R., 1997. An Introduction to Error Analysis, 2nd Edn., University Science Books, Sausalito, CA.

Trent, E.M., 1991. Metal Cutting. Butterworth/ Heinemann, London.

Yallese, M.A., K. Chaoui, N. Zeghib, L. Boulanouar and J. Rigal, 2009. Hard machining of hardened bearing steel using cubic boron nitride tool. J. Mater. Proc. Tech., 209: 1092-1104.

Wyatt, J.E. and J. Berry, 2006. A new technique for the determination of superficial residual stresses associated with machining and other manufacturing processes. J. Mater. Proc. Tech., 171: 132-140.